Hypoxanthine as an Inhibitor for Mild Steel Corrosion in 0.1 M HCl

Habibat Momoh-Yahaya[1*] Nnabuk Eddy[2] Johnson Iyun[2] Casmir Gimba[2] Emeka Oguzie[3]

1. Department of Chemistry, University of Agriculture Makurdi, P.M.B. 2373, Makurdi, Nigeria
2. Department of Chemistry, Ahmadu Bello University Zaria, Nigeria
3. Electrochemistry and Materials Science Research Laboratory, Department of Chemistry, Federal University of Technology Owerri, PMB 1526, Owerri, Nigeria

* E-mail of the corresponding author: momohbat2007@gmail.com

Abstract

Hypoxanthine (HYP) has been evaluated as a corrosion inhibitor for mild steel in aerated 0.1 M hydrochloric acid by weight loss, potentiodynamic polarisation and electrochemical impedance spectroscopy techniques at 30 and 60 °C respectively. The results showed that hypoxanthine is a moderate inhibitor in the acidic medium. Potentiodynamic polarisation results revealed hypoxanthine to be a mixed inhibitor. Inhibition efficiency increased with increase in the concentrations of hypoxanthine but decreased with a rise in temperature of 60 °C . The adsorption of the inhibitor on the mild steel surface is found to obey Langmuir adsorption isotherm. From the values of E_a and $G°_{ads}$ obtained, the mechanism of physical adsorption is proposed for the inhibitive action of hypoxanthine.

Key Words: acid solutions, adsorption, inhibition efficiency, potentiodynamic polarisation

1.Introduction

Corrosion of metals is a major industrial problem that has attracted much investigation and researches (Oguzie, 2004; Chetounani et.al., 2004., Monika and Sidique, 2005). Corrosion is the primary means by which metals deteriorate. Most metals corrode on contact with water (and moisture in the air), acids, bases, salts, oils, aggressive metal polishes, and other solid and liquid chemicals. The corrosion of steel in acidic solution is the most common form of corrosion and has practical importance during industrial processes such as acid pickling of iron and steel, chemical cleaning of the scale in metallurgy, oil recovery in the petroleum industries, etc (Bouyanzer and Hammouti, 2004; Ebenso et.al., 2008; Obot et.al., 2009; Eddy et.al., 2010).

The rate of corrosion of mild steel depends on the concentration of acids, temperature, period of contact, the presence or absence of an inhibitor, etc (Quraishi and Jamal, 2002; Abdallah, 2004; Ashassi-Sorkhabi et.al., 2006; Umoren and Ekanem, 2010).

Because of the general aggression of acid solutions, inhibitors are commonly used to reduce the corrosive attack on metallic materials. Inhibitors allow the reduction of corrosion rate by influencing the kinetics of corrosion processes which are consistent with anodic and cathodic conjugate reactions.

Among most well known acid inhibitors, nitrogen-containing heterocyclic compounds are considered to be effective corrosion inhibitors (Bentiss et.al., 2000). N-heterocyclic compound inhibitors act by adsorption on the metal surface through the nitrogen heteroatom, as well as those with triple or conjugated double bonds or aromatic rings in their molecular structures. Inhibitor adsorption on mild steel in acid solutions usually leads to a structural modification in the double layer with subsequent reduction in the rates of the electrochemical half-cell reactions—the anodic metal dissolution and the cathodic reduction of hydrogen ions (Li et.al., 2009).

Purine (PU) and purine derivatives are nontoxic and biodegradable making the investigation of there inhibiting properties significant in the context of the current priority to produce "green" or environmentally "friendly" inhibitors. Scendo obtained interesting and good results concerning the use of adenine and purine as effective corrosion inhibitors for copper in neutral media (Scendo, 2007a; Scendo, 2007b, Scendo, 2008). Amin *et al.* (2008) investigated the synergistic effect of I^- ions on the corrosion of Aluminium in 1.0 M phosphoric acid solutions by purine, while,Yan *et al.* (2008) did an electrochemical, weight loss and quantum chemical study of some selected purines as corrosion inhibitors for mild steel in 1M HCl solution. The compounds studied were guanine, adenine, 2,6-diamiopurine, 6-thioguanine and 2,6-dithiopurine. The results of their studies showed purines to act as mixed and moderate inhibitors.

The present study investigates the inhibition mechanism of hypoxanthine on mild steel corrosion in hydrochloric acid solution using weight loss and electrochemical techniques. In addition to providing information on the corrosion rate, electrochemical techniques are well suited for monitoring in situ any perturbation by an inhibitor with respect to electrochemical processes in the metal/corrodent interface.

2. Experimental

2.1 Materials

Metal sheets of composition (wt.%: Mn (0.6), P (0.36), C (0.15), Si (0.03) and the rest Fe) were used in this study. The purine derivative was obtained from Zayo-Sigma Chemicals. Figure 1 shows the molecular structure of Hypoxanthine (HYP). The aggressive solution of 0.1 M HCl was prepared by diluting analytical grade with distilled water while inhibitor test solutions were prepared in the concentration range 2.0 x 10^{-3} – 10.0 x 10^{-3} M in 0.1 M HCl solution.

2.2 Weight loss Measurements

Gravimetric experiments were conducted on test coupons of dimension 5 x 4 x 0.15 cm. These were prepared and cleaned as described elsewhere (Oguzie et.al., 2010; Eddy et.al., 2011). The precleaned and weighed coupons were suspended in beakers containing the test solutions using glass hooks and rods. Tests were conducted under total immersion conditions in 250 mL of the aerated and unstirred test solutions. To determine weight loss with respect to time, the coupons were retrieved from test solutions at 24-h intervals, appropriately cleaned, dried, and reweighed. The weight loss was taken to be the difference between the weight of the coupons at a given time and its initial weight. All tests were run in duplicates and the data showed good reproducibility. Average values for each experiment were obtained and used in subsequent calculations.

2.3 Electrochemical Measurements

Metal samples of 2.0 cm x 2.0 cm x 0.15 cm were abraded with a series of silicon carbide abrasive paper (from grade no. 400 to 1200), rinsed with distilled water, degreased in ethanol and dried in acetone. Electrochemical experiments were conducted in a Model K0047 corrosion cell using a VERSASTAT 400 complete DC voltammetry and corrosion system, with V3 Studio software. A graphite rod was used as a counter electrode and a saturated calomel electrode (SCE) as a reference electrode. The latter was connected via a Luggin capillary. Measurements were performed in aerated and unstirred solutions at the end of 1 h of immersion at 30 °C ± 1. Impedance measurements were made at corrosion potentials (E_{corr}) over a frequency range of 100 kHz– 10 mHz, with a signal amplitude perturbation of 5 mV. Potentiodynamic polarization studies were carried out in the potential range ±250 mV versus corrosion potential at a scan rate of 0.33 mV/s. Each test was run in triplicate to verify the reproducibility of the data (Oguzie et.al., 2009).

2.4 Scanning Electron Microscopy (SEM)

Morphological studies of the mild steel electrode surfaces exposed to uninhibited and inhibited 0.1 M HCl solutions for 3 h at 30 °C were undertaken by using a Jeol JSM-7500F scanning electron microscope.

3. Results and Discussion

3.1 Gravimetric Data

The inhibitive effect of HYP on the corrosion of mild steel in 0.1 M HCl was investigated using gravimetric technique. Figure 2 illustrates the weight loss of carbon steel in uninhibited and inhibited

0.1 M HCl as a function of exposure time. The results show that HYP diminished the corrosion rates of mild steel in the acid environment.

Corrosion rate increased with immersion time for both inhibited and uninhibited systems but decreased steadily with increasing HYP concentration. The inhibiting effect of HYP on mild steel corrosion was quantified by evaluating the inhibition efficiency IE (%) as follows:

$$IE\% = \left(1 - \frac{\Delta W_{inh}}{\Delta W_{blank}}\right) X100 \quad (1)$$

where ΔW_{inh} and ΔW_{blank} represent weight losses in inhibited and uninhibited solution, respectively.

Figure 3 illustrates the corresponding trend of inhibition efficiency for various concentrations of HYP at 30 and 60 °C, and as expected, efficiency increased steadily with HYP concentration in the acid medium with the highest inhibition efficiency of 70.84% with 0.01 M HYP at 30 °C.

3.2 Electrochemical Measurements

Electrochemical impedance spectroscopy and potentiodynamic polarization measurements were carried out at 30 °C to understudy the inhibiting effect of HYP (0.01 M) on the corrosion behavior of mild steel in 0.1 M HCl from an electrochemical perspective.

3.2.1 Electrochemical Impedance Spectroscopy Data

The corrosion behaviour of mild steel in 0.1 M HCl in the absence and presence of HYP were investigated by electrochemical impedance spectroscopy after immersion for 30 mins at 303 ± 1 K. Nyquist plots for mild steel corrosion in 0.1 M HCl in the absence and presence of 0.01 M HYP is given in Figure 4. The Nyquist plot show single semicircle over the frequency range studied, corresponding to one time constant in the Bode plot. The increased diameter of capacitive loop obtained in 0.1 M HCl in presence of HYP indicate the inhibition of corrosion of mild steel. The high frequency intercept with the real axis in the Nyquist plot is assigned to the solution resistance (R_s) and the low frequency intercept with the real axis is ascribed to the charge transfer resistance (R_{ct}). The impedance spectra were analyzed by fitting to the equivalent circuit model $R_s(Q_{dl}R_{ct})$, which has been used previously to adequately model the mild steel/acid inter- face (Oguzie et.al., 2009; Quraishi and Singh, 2010). In this equivalent circuit, the solution resistance is shorted by a constant phase element (CPE) that is placed in parallel to the charge transfer resistance. The CPE is used inplace of a capacitor to compensate for deviations from ideal dielectric behavior arising from the inhomogeneous nature of the electrode surfaces. The impedance of the CPE is given by

$$Z_{CPE} = Q^{-1}(j\omega)^{-n} \tag{2}$$

where Q and n stand for the CPE constant and exponent, respectively, $j = (-1)^{1/2}$ is an imaginary number, and ω is the angular frequency in rad s^{-1} ($\omega = 2\pi f$), where f is the frequency in Hz.

The corresponding electrochemical parameters are presented in Table 2 and reveal that HYP increased the magnitude of R_{ct}, with corresponding decrease in the double layer capacitance (Q_{dl}). The increase in R_{ct} value in the inhibited system, which corresponds to an increase in the diameter of the Nyquist semicircle, confirms the corrosion inhibiting effect of HYP. The observed decrease in C_{dl} values, which normally results from a decrease in the dielectric constant and/or an increase in the double-layer thickness, can be attributed to the adsorption of HYP (with lower dielectric constant compared to the displaced adsorbed water molecules) onto the metal/electrolyte interface, thereby protecting the metal from corrosive attack .

Inhibition efficiency from the impedance data (IE_R%) was estimated by comparing the values of the charge transfer resistance in the absence (R_{ct}) and presence of inhibitor ($R_{ct,inh}$) as follows:

$$IE\% = \left(\frac{R_{ct(inh)} - R_{ct}}{R_{ct(inh)}}\right) \times 100 \tag{3}$$

Corrosion kinetic parameters derived from EIS measurements and inhibition efficiencies are given in Table 2.

3.2.2 Potentiodynamic Polarization Data

Potentiodynamic polarization experiments were undertaken to distinguish the effect of HYP on the anodic dissolution of mild steel and cathodic hydrogen ion reduction. Typical potentiodynamic polarization curves for mild steel in 0.1 M HCl in the absence and presence of HYP are shown in Figure 5, while the electrochemical parameters derived from the polarization curves are summarized in Table 3. It can be observed that both the cathodic and anodic reactions were suppressed with the addition of HYP, which suggests that HYP affected the anodic as well as the cathodic partial reactions, shifting the corrosion potential (E_{corr}) slightly toward more positive (anodic) values and reducing the anodic and cathodic current densities and the corresponding corrosion current density (i_{corr}). This indicates that the extracts functioned as a mixed-type inhibitor in the acid solution. The values of the corrosion current densities in the absence

(i_{corr}) and presence of inhibitor ($i_{corr,inh}$) were used to estimate the inhibition efficiency from polarization data (IE_i%) as follows:

$$IE_i\% = \left(1 - \frac{i_{inh}}{i_{corr}}\right) \times 100 \qquad (4)$$

3.3 Adsorption Isotherm

It is generally agreed that corrosion inhibition is due to the adsorption of the inhibitor molecule at the metal–solution interface, which is accompanied by a change in potential difference between the metal electrode and the solution due to the nonuniform distribution of electric charges at the interface (Sastri, 2011). The adsorbed inhibitor then acts to retard the cathodic and/or anodic electrochemical corrosion reaction. Basic information on the interaction between the inhibitor and the mild steel surface can be provided by the adsorption isotherm. Adsorption of an inhibitor molecule occurs as the interaction energy between molecule and metal surface is higher than that between the H_2O molecule and the metal surface (Quraishi and Singh, 2010). In this study, Langmuir adsorption isotherm was found best for describing the adsorption behaviour of HYP on the mild steel surface in HCl solution , Figure 6. Langmuir adsorption isotherm is described by the following equation:

$$\frac{C}{\theta} = \frac{1}{K_{ads}} + C \qquad (5)$$

where K_{ads} is the equilibrium constant of the adsorption-desorption process, θ is the degree of surface coverage and C is the concentration of inhibitor in the bulk solution.

Figure 6 shows the dependence of the fraction of the surface covered C/θ as a function of the concentration C, of HYP. The obtained plots of the inhibitor are almost linear with a correlation coefficient higher than 0.99. Though linear plots were obtained, the deviations of the slope from unity imply that the isotherm may not be strictly applicable , Table 4. Deviation of the slope from unity suggests interaction between adsorbed molecules on the metal surface as well as changes in the heat of adsorption with increasing surface coverage (Obot and Obi-Egbedi, 2008; Obot and Obi-Egbedi, 2010).

Table 4 shows that the value of the adsorptive equilibrium constant, K_{ads} is lower at a higher temperature which implies that the inhibitor tend to desorb from the mild steel at 60 °C resulting in lower inhibition efficiency values. Calculated values of ΔG_{ads} are negative and less than -40 KJ/mol, this indicates that the adsorption of HYP on the mild steel surface is spontaneous and proceeded via physical adsorption mechanism (Eddy and Ebenso, 2010).

3.4 Thermodynamic considerations

The corrosion process kinectics acquire the character of a diffusion process, in which at a higher temperature, the amount of inhibitor molecules present at the metal surface is lower than at a lower temperature. The enhancement of inhibition effeiciency at a lower temperature may be due to high activation energy available for adsorption. The apparent activation energies (E_a) for the corrosion

process in absence and presence of HYP were evaluated from a modified form of the Arrhenius equation:

$$log\frac{\rho_2}{\rho_1} = \frac{E_a}{2.303R}\left(\frac{1}{T_1} - \frac{1}{T_2}\right) \qquad (6)$$

Where ρ_1 and ρ_2 are the corrosion rates at temperatures T_1 and T_2, respectively. An estimate of the heats of adsorption (Q_{ads}) was obtained from the trend of surface coverage with temperature as follows [19]:

$$\mathrm{Q_{ads}} = 2.303\mathrm{R}\left[\log\left(\frac{\theta_2}{1-\theta_2}\right) - \log\left(\frac{\theta_1}{1-\theta_1}\right)\right] \times \frac{\mathrm{T_1T_2}}{\mathrm{T_2-T_1}} \qquad (7)$$

where θ_1 and θ_2 are the degrees of surface coverage at temperatures T_1 and T_2, and R is the gas constant. The calculated values for both parameters are given in Table 5.

The equilibrium constant of adsorption K_{ads} is related to the standard free energy of adsorption ΔG_{ads}, by the following equation

$$K_{ads} = \frac{1}{55.5} exp^{\frac{-\Delta G^{\circ}_{ads}}{RT}} \qquad (8)$$

where R is the molar gas constant, T is the absolute temperature and 55.5 is the concentration of water in solution expressed in M.

Rearranging Eq. (8) gives:

$$logK_{ads} = -1.744 - \frac{\Delta G^{\circ}_{ads}}{2.303RT} \qquad (9)$$

from where the standard free energy of adsorption can be calculated. The calculated ΔG_{ads} and K_{ads} values are listed in Table 4.

The negative Q_{ads} in values in Table 5 also signify that the degree of surface coverage decreased with rise in temperature. The reason for this may be due to the fact that the attainment of physical adsorption equilibrium is usually rapid and the process readily reversible whereas in chemisorptions, the occurrence of chemical reactions at the metal surface makes the process relatively slow and not readily reversible (Oguzie, 2004).

3.5 SEM Surface Examination

Morphological studies of the surfaces of mild steel specimens in uninhibited and inhibited acid solutions were carried out by SEM after immersion in the different test solutions for 3 h at 30 °C. Figure 7 shows the SEM images of the mild steel surface after 3 h immersion in uninhibited 0.1 M HCl (Figure 7a) and the presence of 0.01 M HYP (Figure 7b). A severely corroded surface morphology is observed after immersion in the uninhibited system, due to corrosive attack of the acid solution (Figures 7a). Corrosion was relatively general with no evidence of localized attack. The corrosion product layer on the metal surface in uninhibited 0.1 M HCl (Figure 7a) is clearly very loose and porous and would thus offer insignificant corrosion protection.

With addition of HYP (Figure 7b), the corrosion damage is visibly reduced, and there is slight evidence of the adsorbate presence on the metal surface.

4.Conclusion

Hypoxanthine acts as an inhibitor for the corrosion of mild steel in 0.1 M HCl. Inhibition efficiency of hypoxanthine decreased with temperature, resulting in an increase in activation energy of the corrosion process. The adsorption of hypoxanthine on mild steel surface from 0.1 M HCl obeys the Langmuir adsorption isotherm. Phenomenon of physical adsorption is proposed from the values of (E_a, Q_{ads}, ΔG°_{ads}) obtained. Potentiodynamic curves shows that hypoxanthine functions as a mixed-type inhibitor.

References

Chetounani, A. et al. (2004). Corrosion Inhibition of Iron in Hydrochloric Acid Solution by Jojoba Oil. *Pigment and Resin Technology*. 33, 26-31.

Oguzie, E.E. (2004). Influence of Halide Ions on the Inhibitive Effect of Congo Red Dye on the Corrosion of Mild Steel in Sulphuric Acid Solution. *Materials Chemistry and Physics*. 87, 212-217.

Monika, W.A., Siddique, A.D. (2005). Inhibiting Effect of N-Cetyl N,N,N-Trimethyl Ammonium Bromide on Corrosion of Mild Steel in Acidic Medium. *Portugaliae Electrochimica Acta*. 23, 445-455.

Bouyanzer, A., Hammouti, B. (2004). A Study of Anti-Corrosion Effects of Artemisia Oil on Steel. *Pigment and Resin Technology*. 33, 287 -292.

Ebenso, E.E., Alemu, H., Umoren, S.A., Obot, I.B. (2008). Inhibition of Mild Steel Corrosion in Sulphuric Acid using Alizarin Yellow GG Dye and Synergistic Iodide Additive. *International Journal Electrochemical Science*. 3, 1325-1339.

Obot, I.B., Obi-Egbedi, N.O., Umoren, S.A. (2009). Corrosion Inhibition and Adsorption Behavior of Clotrimazole on Aluminium in Hydrochloric Acid and Synergistic Effect of Iodide ion . *International Journal of Electrochemical Science*. 4, 863-877.

Eddy, N.O., Ebenso, E.E., Ibok, U.J. (2010). Adsorption, Synergistic Inhibitive Effect and Quantum Chemical Studies on Ampicillin and Halides for the Corrosion of Mild Steel. *Journal of Applied Electrochemistry*. 40, 445-456.

Quraishi, M.A., Jamal, D. (2002). Inhibition of Mild Steel Corrosion in the Presence of Fatty Acid Triazoles . *Journal of Applied Electrochemistry*. 32, 425-430.

Abdallah, M. (2004). Guar Gum as Corrosion Inhibitor for Carbon Steel in Sulphuric Acid Solutions. *Portugaliae Electrochimica Acta* . 22, 161-175.

Ashassi-Sorkhabi, H., Shaabani, B., Aligholipour, B., Seifzadeh, D. (2006). The Effect of Some Schiff Bases on the Corrosion of Aluminium in HCl Solution. *Applied Surface Science* 252, 4039-4047.

Umoren, S.A., Ekanem, U.F. (2010). Inhibition of Mild Steel Corrosion in H_2SO_4 using Exudate Gum from Pachylobus Edulis and Synergistic Potassium Halides Additives. *Chemical Engineering Communications*. 197, 1339-1356.

Bentiss, F., Traisnel, M., Gengembre, L., Lagrenée, M. (2000). Inhibition of Acidic Corrosion of Mild Steel by 3,5-Diphenyl-4*H*-1,2,4-Triazole. *Applied Surface Science*. 161, 194-202.

Li, X., Deng, S., Fu, H., Li, T. (2009). Adsorption and Inhibition Effect of 6-Benzylaminopurine on Cold Rolled Steel in 1.0 M HCl. *Electrochimica Acta*. 54, 4089-4098.

Scendo, M. (2007). The Effect of Purine on the Corrosion of Copper in chloride solutions. *Corrosion Science*. 49, 373-390.

Scendo, M. (2007). Inhibitive Action of Purine and Adenine for Copper Corrosion in Sulphate Solutions. *Corrosion Science*. 49, 2985-3000.

Scendo, M. (2008). The Influence of Adenine on Corrosion of Copper in Chloride Solutions. *Corrosion Science*. 50, 2070–2077.

Amin, M.A., Mohsen, Q., Hazzazi, O.A. (2008). Synergistic Effect of I^- Ions on the Corrosion Inhibition of Al in 1.0 M Phosphoric Acid Solutions by Purine. *Materials Chemistry and Physics* doi: 10.1016/j.matchemphys.2008.10.057.

Yan, Y., Weihua, L., Lankun, C., Baorong, H. (2008). Electrochemical and Quantum Chemical Study of Purines as Corrosion Inhibitors for Mild Steel in 1 M HCl Solution. *Corrosion Science*. 53, 5953-5960.

Oguzie, E.E. et al. (2010). Adsorption and Corrosion Inhibiting Effect of Dacryodis Edulis Extract on Low Carbon Steel Corrosion in Acidic Media. *Journal of Colloid and Interface Science*. 349, 283-292.

Eddy, et al. (2011). QSAR, Experimental and Computational Chemistry Simulation Studies on the Inhibition Potentials of Some Amino Acids for the Corrosion of Mild Steel in 0.1 M HCl. *International Journal of Electrochemical Science*. 6, 931-957.

Oguzie, E.E., Wang, S.G., Li Y., Wang, F.H. (2009). Influence of Iron Microstructure on Corrosion Inhibitor Performance in Acidic Media. *Journal of Physical Chemistry C*. 113, 8420-8429.

Singh, A.K., Quraishi, M.A. (2010). Piroxicam; A Novel Corrosion Inhibitor for Mild Steel Corrosion in HCl Acid Solution. *Journal of Materials and Environmental Science*. 1,101-110.

Sastri, V.S. (2011). Green Corrosion Inhibitors: Theory and Practice. John Wiley and Sons, Inc., Hoboken, New Jersey.

Obot, I.B., Obi-Egbedi, N.O. (2008). Fluconazole as an Inhibitor for Aluminium Corrosion in 0.1M HCl. *Colloids and Surfaces A: Physicochemical Engineering Aspects.* 330, 207–212.

Obot, I.B., Obi-Egbedi, N.O. (2010). Adsorption Properties and Inhibition of Mild Steel Corrosion in Sulphuric Acid Solution by Ketoconazole: Experimental and Theoretical Investigation. *Corrosion Science*. 52, 198–204.

Eddy, N.O., Ebenso, E.E. (2010). Adsorption and Quantum Chemical Studies on Cloxacillin and Halides for the Corrosion of Mild Steel in Acidic Medium. *International Journal of Electrochemical Science*. 5, 731 – 750.

Oguzie, E.E. (2004). Influence of Halide Ions on the Inhibitive Effect of Congo Red Dye on the Corrosion of Mild Steel in Sulphuric Acid Solution. *Materials Chemistry and Physics.* 87, 212-217.

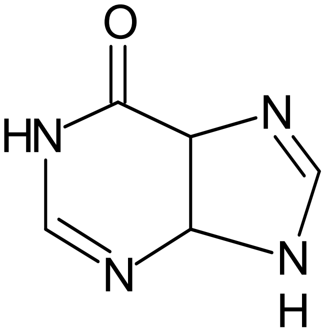

Figure 1. Molecular structure of hypoxanthine

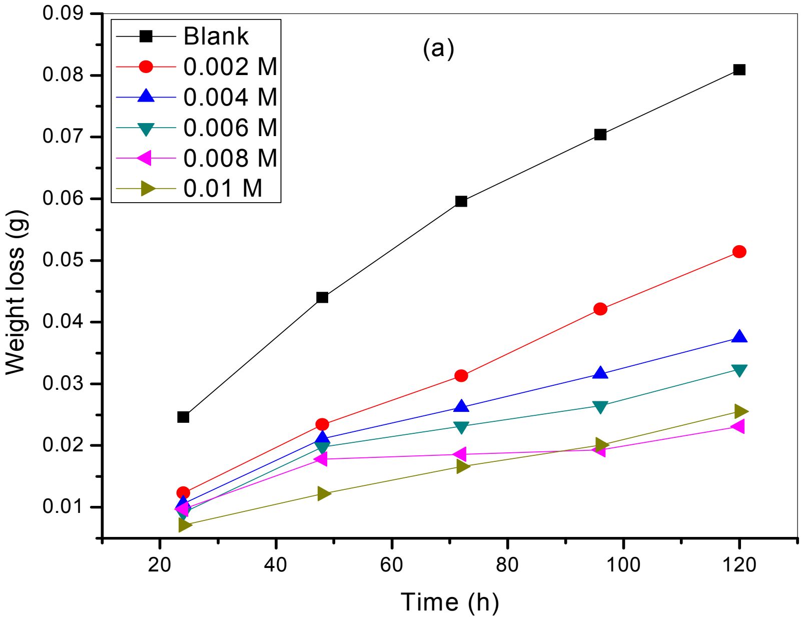

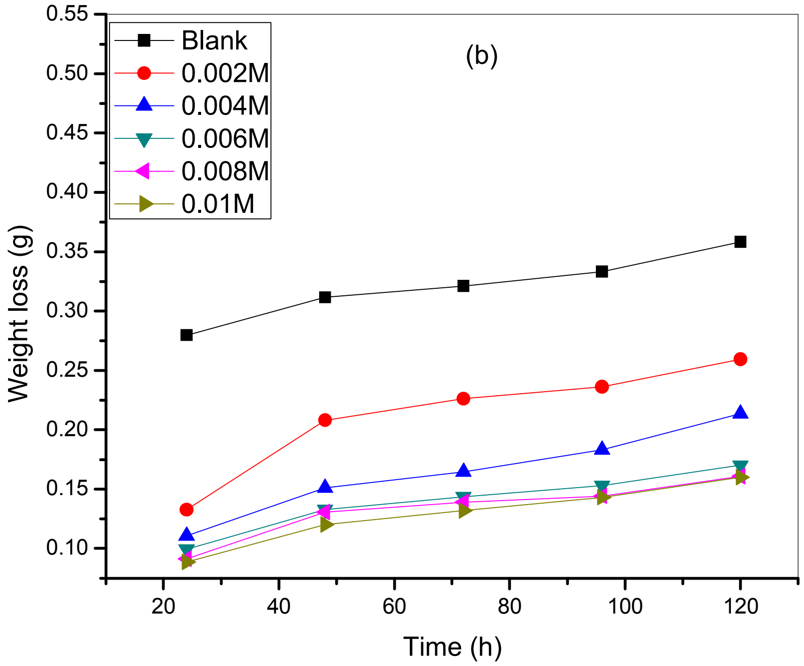

Figure 2. Weight losses of mild steel in 0.1 M HCl solution without and with different concentrations of HYP at (a) 30 °C and (b) 60 °C .

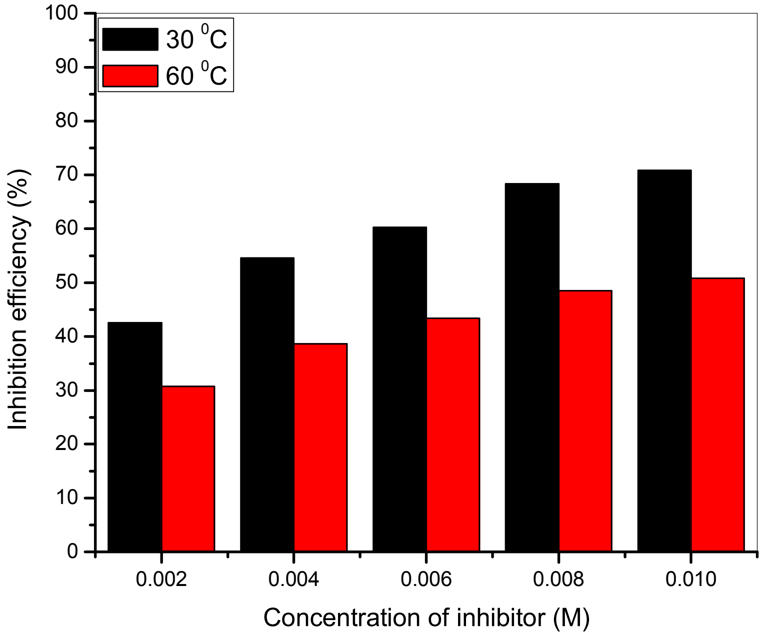

Figure 3. Variation of IE % with different concentrations of HYP in 0.1 M HCl at 30 °C and 60 °C respectively..

Table 1. Corrosion parameters for mild steel in 0.1 M HCl in the absence and presence of different concentrations of HYP at 30 °C and 60 °C respectively.

Temperature °C	**System/Concentration (M)**	**Corrosion rate x 10^{-4} ($gh^{-1}cm^{-2}$)**	**IE %**	**Surface coverage θ**
30	Blank	1.16		
	0.002	0.67	42.58	0.43
	0.004	0.53	54.56	0.55
	0.006	0.46	60.29	0.61
	0.008	0.37	68.33	0.68
	0.01	0.34	70.84	0.71
60	Blank	6.68		
	0.002	4.63	30.70	0.31
	0.004	4.10	38.65	0.39
	0.006	3.78	43.42	0.43
	0.008	3.44	48.47	0.49
	0.01	3.29	50.81	0.51

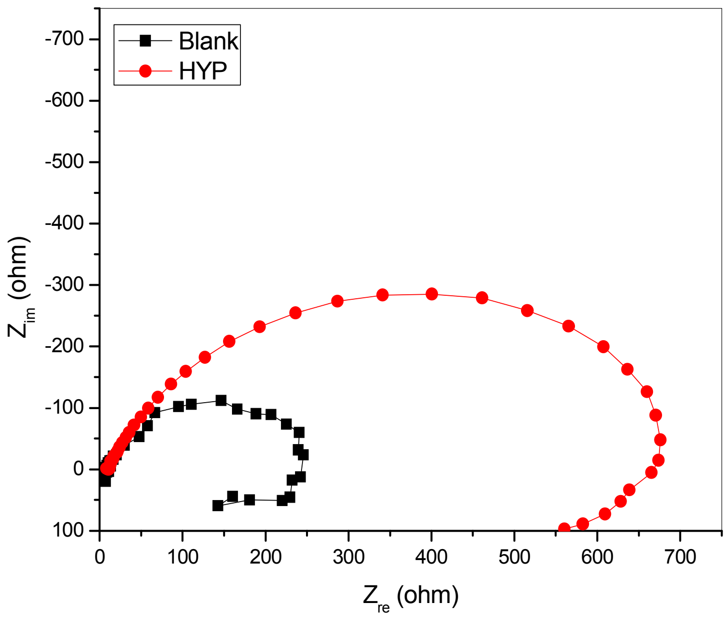

Figure 4. Electrochemical impedance spectra of mild steel in 0.1 M HCl in the absence and presence of 0.01 M HYP.

Table 2. Electrochemical impedance parameters for mild steel in 0.1 M HCl in the absence and presence of 0.01 M HYP.

System/Concentration	R_{ct} (Ω cm^2)	C_{dl} ($\mu\Omega^{-1}S^n cm^{-2}$)	N	IE%
HCl	231.4	3.5	0.87	-
HYP (0.01 M)	689.8	0.39	0.82	66.45

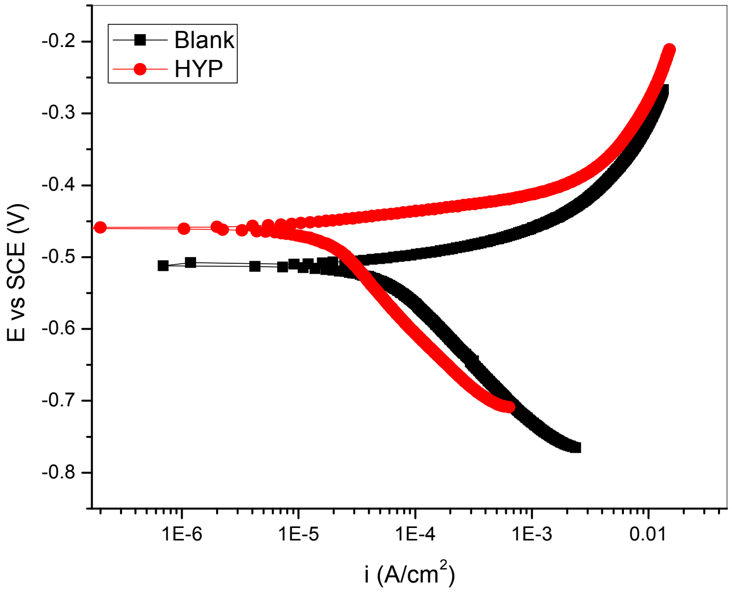

Figure 5. Potentiodynamic polarization curves of mild steel in 0.1 M HCl in the absence and presence of 0.01 M HYP.

Table 3. Potentiodynamic polarization parameters for mild steel in 0.1 M HCl in the absence and presence of 0.01 M HYP.

System	E_{corr} (mV vs SCE)	i_{corr} (μA/cm^2)	IE%
HCl (Blank)	-512.13	173.1	
HYP (0.01 M)	-459.78	57.59	66.73

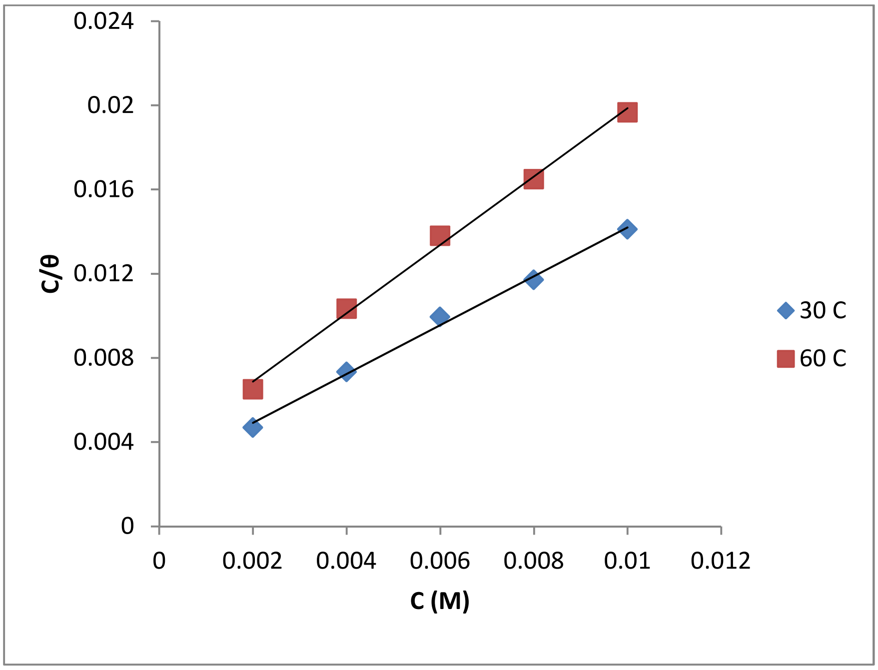

Figure 6. Langmuir isotherm for the adsorption of HYP in 0.1 M HCl at 30 and 60 °C.

Table 4. Calculated thermodynamic parameters from Langmuir adsorption isotherm.

Temperature °C	Intercept	Slope	Kads (M^{-1})	R^2	$\Delta G°_{ads}$ $kJmol^{-1}$
30	0.002	1.16	500	0.995	-25.78
60	0.003	1.624	333	0.996	-24.75

Table 5. Calculated values of activation energy (E_a) and heat of adsorption (Q_{ads}) for mild steel dissolution in 0.1 M HCl in the absence and presence of HYP.

System/Concentration (M)	E_a $kJmol^{-1}$	Q_{ads} $kJmol^{-1}$
Blank	49.02	
0.002	54.16	-5.44
0.004	57.33	-6.82
0.006	58.79	-7.21
0.008	62.50	-8.78
0.01	63.54	-8.77

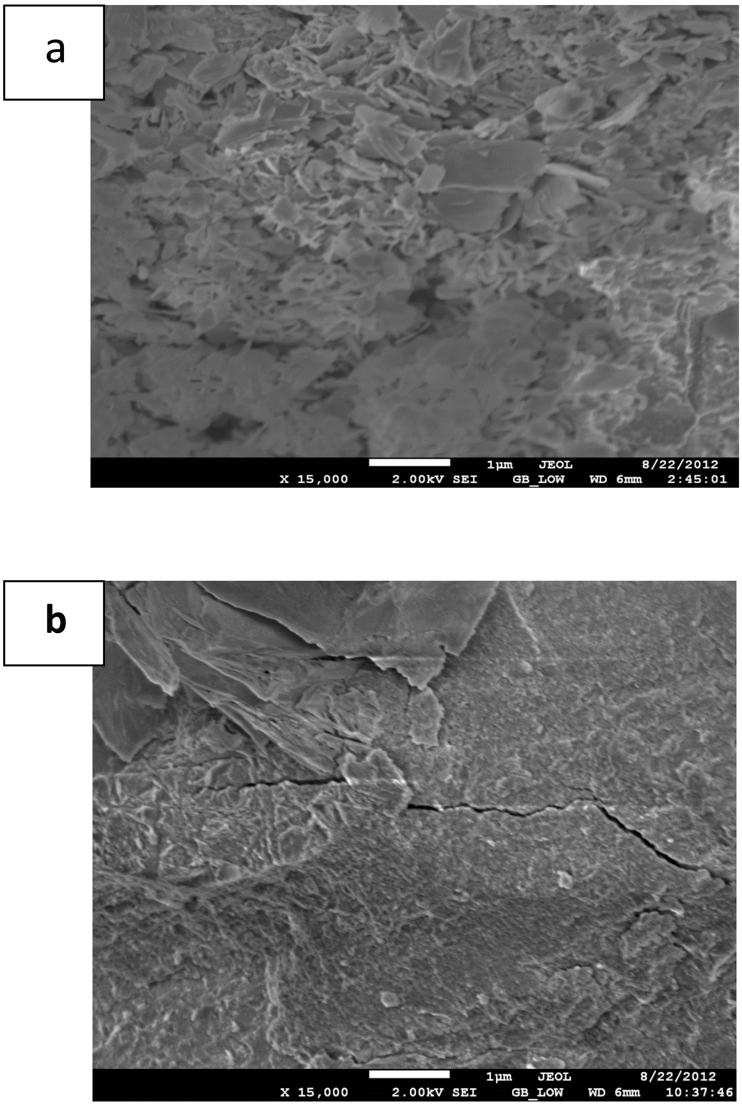

Figure 7. SEM images of mild steel surface after 3 h immersion at 30 °C in 0.1 M HCl: (a) without HYP and (b) with 0.01 M HYP.

This academic article was published by The International Institute for Science, Technology and Education (IISTE). The IISTE is a pioneer in the Open Access Publishing service based in the U.S. and Europe. The aim of the institute is Accelerating Global Knowledge Sharing.

More information about the publisher can be found in the IISTE's homepage: http://www.iiste.org

The IISTE is currently hosting more than 30 peer-reviewed academic journals and collaborating with academic institutions around the world. **Prospective authors of IISTE journals can find the submission instruction on the following page:** http://www.iiste.org/Journals/

The IISTE editorial team promises to the review and publish all the qualified submissions in a fast manner. All the journals articles are available online to the readers all over the world without financial, legal, or technical barriers other than those inseparable from gaining access to the internet itself. Printed version of the journals is also available upon request of readers and authors.

IISTE Knowledge Sharing Partners

EBSCO, Index Copernicus, Ulrich's Periodicals Directory, JournalTOCS, PKP Open Archives Harvester, Bielefeld Academic Search Engine, Elektronische Zeitschriftenbibliothek EZB, Open J-Gate, OCLC WorldCat, Universe Digtial Library , NewJour, Google Scholar